Published in final edited form as:
Nature. 2009 July 9; 460(7252): 259–263. doi:10.1038/nature08099.

Bone marrow adipocytes as negative regulators of the hematopoietic microenvironment

Olaia Naveiras[1], **Valentina Nardi**[1,*], **Pamela L. Wenzel**[1,*], **Frederic Fahey**[2], and **George Q. Daley**[1,3]

[1]Division of Pediatric Hematology/Oncology, Children's Hospital Boston and Dana Farber Cancer Institute; Department of Biological Chemistry and Molecular Pharmacology, Harvard Medical School; Division of Hematology, Brigham and Women's Hospital; Harvard Stem Cell Institute, Boston, MA 02115; Manton Center for Orphan Diseases; Howard Hughes Medical Institute

[2]Department of Radiology, Division of Nuclear Medicine/PET, Children's Hospital Boston, Harvard Medical School, 300 Longwood Ave, Boston, MA, 02115, USA

Abstract

Osteoblasts and endothelium constitute functional niches that support hematopoietic stem cells (HSC) in mammalian bone marrow (BM) 1‚2‚3 . Adult BM also contains adipocytes, whose numbers correlate inversely with the hematopoietic activity of the marrow. Fatty infiltration of hematopoietic red marrow follows irradiation or chemotherapy and is a diagnostic feature in biopsies from patients with marrow aplasia 4. To explore whether adipocytes influence hematopoiesis or simply fill marrow space, we compared the hematopoietic activity of distinct regions of the mouse skeleton that differ in adiposity. By flow cytometry, colony forming activity, and competitive repopulation assay, HSCs and short-term progenitors are reduced in frequency in the adipocyte-rich vertebrae of the mouse tail relative to the adipocyte-free vertebrae of the thorax. In lipoatrophic A-ZIP/F1 "fatless" mice, which are genetically incapable of forming adipocytes8, and in mice treated with the PPARγ inhibitor Bisphenol-A-DiGlycidyl-Ether (BADGE), which inhibits adipogenesis9, post-irradiation marrow engraftment is accelerated relative to wild type or untreated mice. These data implicate adipocytes as predominantly negative regulators of the bone marrow microenvironment, and suggest that antagonizingmarrow adipogenesis may enhance hematopoietic recovery in clinical bone marrow transplantation.

At birth, hematopoietic red marrow occupies virtually the entirety of the bone marrow space, but with age, non-hematopoietic fatty marrow gradually predominates 4. This so-called "fatty degeneration" of the marrow is a dynamic and reversible process 5‚6. To investigate whether marrow adipocytes influence hematopoiesis, we surveyed the mouse skeleton for bones that harbour fatty marrow under normal conditions. We found that the spine of adult mice manifests a proximal to distal gradient of bone marrow adipocytes: thoracic vertebrae are virtually adipocyte-free, while vertebrae starting at the level of the third or fourth tail segments are highly adipocytic (figure 1a). We isolated bone marrow from the thoracic and tail vertebrae of 12 week-old mice and quantified the hematopoetic stem cell and short-term progenitor compartments both phenotypically and functionally (schema in supplementary

[3]Corresponding author: George Q. Daley, Division of Hematology/Oncology, Children's Hospital Boston, 300 Longwood Avenue – Karp 7th, Boston, MA 02115, Phone: 617 970 0216 / Fax: 617 730 0222, Email: george.daley@childrens.harvard.edu.
[*]These authors have contributed equally to this work

Author Contributions: O.N and G.Q.D. conceived the original idea, designed experiments and wrote the manuscript. O.N., V.N. and P.W. performed experiments and analyzed results. O.N. and F.F. performed quantitative acquisition and analysis of mCT and mPET. All authors edited and reviewed the final manuscript.

figure 1). BM from tail vertebrae contains only 25% as many CD45+ hematopoietic cells per segment as thoracic BM, thus confirming the reduced overall hematopoietic cellularity evident by histology (figure 1b, supplementary figure 2a). Using flow cytometry, we determined the relative frequency of hematopoietic stem cells (HSC, ckit+Sca1+Lin-Flk2- or KLSF), multipotent progenitors (MPP), common myeloid progenitors (CMP), granulocyte-monocyte progenitors (GMP), and megakaryocyte-erythroid progenitors (MEP) in these different regions of the spine 10. The percentage of all progenitor classes was reduced 2–3 fold in the CD45+ hematopoietic cells of adipocyte-rich BM of the tail vertebrae compared to non-adipocytic BM from the thoracic vertebrae (figure 1c, supplementary figure 2b). Congruent with the FACS phenotype data, long-term repopulating HSCs, short-term repopulating progenitors, spleen colonies and methylcellulose colony forming units were reduced 1.5–3 fold in adipocyte-rich BM from tail vertebrae as compared to adipocyte-free BM from the thoracic vertebrae (figure 1d–1f, supplementary figure 2c). These phenomena are neither due to age nor weight-bearing status, for we observed a similar reduction in the frequency of short-term progenitors in younger (4 week-old) and older mice (13 months), as well as in another consistently fatty yet weight-bearing region of the mouse skeleton, the distal tibia (supplementary figures 3a–3f). Reduced frequency of CMPs and primitive CFUs also accompany the increased BM adiposity of femurs from leptin deficient obese mice (supplementary figure 4a–4d). Moreover, we found that BM-derived adipocytes reduce the expansion of hematopoietic cells in stromal transwell co-cultures, indicating that adipocytes release diffusible inhibitors of hematopoiesis (supplementary figure 5a–5d). We therefore conclude that adipocyte-rich marrow is associated with lower absolute levels and relative numbers of hematopoietic progenitors.

To investigate the mechanism of reduced hematopoietic activity of adipocytic BM, we performed cell cycle analysis of the progenitor compartments. In all cases, we found fewer progenitors in the replicating phases of the cell cycle (S/G2/M) within the adipocyte-rich BM (figure 1g, supplementary figure 6a). Early progenitors (HSC/MPP) presented no significant difference in their G_0/G_1 ratio, while late progenitors (GMP/CMP/MEP) presented a significant increase in the G_0/G_1 ratio (supplementary figure 6b). To determine if the slow-cycling HSCs within the tail BM were functional, as opposed to senescent, we FACS-sorted HSCs (ckit+Lin-Sca1+Flk2-, KLSF) and transplanted them competitively into lethally irradiated mice. We observed no difference in repopulating activity between HSCs from tail and thorax in the first month post-transplant. However, multilineage long-term engraftment was significantly higher in HSCs purified from tail BM (figure 1h), suggesting that the slow-cycling progenitors in adipocytic tail BM are relatively quiescent and not senescent. This is consistent with the relative predominance of CD34low HSCs within the KLSF fraction of tail BM (figure 1i), a phenotype associated with long–term repopulation activity 11. Taken together, our data establish tail vertebrae as a model for the study of fatty marrow in the mouse, and demonstrate that adipocyte-rich marrow manifests altered hematopoiesis. HSCs and short-term progenitors are functionally reduced on a per cell basis in fatty marrow due to reduced cycling at the level of the HSC, MPP and CMP compartments.

To determine if the association between adipocytic marrow and reduced hematopoietic progenitor frequency is purely correlative, or whether adipocytes actively compromise hematopoiesis, we studied the lipoatrophic “fatless” A-ZIP/F1 mouse, which cannot form adipocytes due to the expression of a dominant negative form of C/EBP under the adipocyte fatty-acid binding protein 4 (aP2/FABP4) promoter 8. In contrast to wildtype mice, we found that the absence of adipocytes in fatless A-ZIP/F1 mice rescued hematopoiesis in the tail, such that A-ZIP/F1 mice presented no significant difference in the frequency of CFUs from thorax or tail BM (supplementary figure 7a–b), indicating that compromised osteogenesis due to the non-weight-bearing nature of these bones cannot explain the

hematopoietic defect of wildtype, adipocyte-rich tail vertebrae 12. Importantly, although fatless A-ZIP/F1 mice are diabetic, their blood counts were similar to controls during homeostasis, and their femoral BM showed no competitive advantage over BM from wild-type littermates, arguing that the diabetic milieu does not account for the observed alterations in the hematopoietic compartment (supplementary figures 8a–c). We therefore conclude that the presence of adipocytes is necessary to observe reduced hematopoiesis in adipocyte-rich tail bone marrow.

We then analyzed the effect of adipocytes on hematopoietic recovery following bone marrow transplantation. Between the second and fourth week after lethal irradiation, the bone marrow space throughout the mouse skeleton becomes replaced by adipocytes. During this post-transplant period mice (and human patients) depend on fast cycling, short-term hematopoietic progenitors to rescue their otherwise lethal pancytopenia 13. Given our prior data, we predicted that the compromised adipogenesis in the A-ZIP/F1 mouse would enhance hematopoietic recovery in the post-transplant period through increased proliferation of short-term progenitors. We transplanted wildtype BM (CD45.2) into either wildtype or fatless A-ZIP/F1 littermates (CD45.1, figure 2a). In contrast to control mice, A-ZIP/F1 fatless mice exposed to lethal doses of irradiation produced markedly fewer adipocytes in the marrow cavity (figure 2b). We monitored leukocyte recovery in the post-transplant period and found that recovering A-ZIP/F1 fatless mice have up to 4 times higher leukocyte counts in peripheral blood relative to their wild-type controls (figure 2c). We also observed significantly accelerated recovery in the hemoglobin content of peripheral blood (figure 2d). Importantly, both wildtype and A-ZIP/F1 fatless recipients showed comparable high-level long-term donor chimerism after the primary transplant (supplementary figure 8d). In the third week post-transplant, we recovered the donor CD45.2 BM from the adipocyte-rich wildtype or the adipocyte-free AZIP/F1 femurs. We found a pronounced increase in hematopoietic progenitors in the recovering CD45.2 BM isolated from fatless A-ZIP/F1 mice as determined by flow cytometry (figure 2e), methylcellulose colony forming assays (figure 2f and supplementary figure 8e) and short-term competitive repopulation into secondary recipients (figure 2g). Collectively, these results indicate that the lack of adipogenesis in A-ZIP/F1 recipient mice enhances hematopoietic recovery after lethal irradiation by enhancing engraftment of short-term progenitors, and further supports the conclusion that adipocytes in fatty marrow hinder hematopoietic progenitor expansion.

During our studies, we observed that bone marrow ablation in lethally irradiated A-ZIP/F1 fatless mice was accompanied by marked osteogenesis. Trabecular bone was increased in the femurs of transplanted A-ZIP/F1 fatless mice compared to wild-type controls (figure 3a), a phenomenon also apparent in the tail and in mice that were lethally ablated but received no transplant (supplementary figures 9a–c). High-resolution micro-Computerized Tomography (mCT) confirmed a 5-fold increase in trabecular bone that was specific to fatless A-ZIP/F1 mice after BM transplantation (figure 3a–c). Incorporation of 18F measured by positron emission tomography (mPET) confirmed an increased bone metabolism, indicating new bone deposition in tails and tibias after bone marrow transplantation that was maximal in the second week post-transplant (figure 3d–e). Our data show that simultaneous ablation of the hematopoietic and BM adipocyte compartment can induce osteogenesis, which, as shown by others, promotes a more supportive environment for hematopoietic reconstitution that could explain the positive effect of adipocyte ablation in BM engraftment 1, 2. Our observation is compatible with a previous report that surgical removal of the fatty marrow in rabbit tibias induces transient hematopoietic infiltration and new osteoid and trabecular bone formation 14. In addition to creating an osteogenic environment, fatless A-ZIP/F1 mice may accumulate mesenchymal elements that support hematopoietic recovery, or may be deficient in osteoclast elements that would antagonize trabecular bone growth during the recovery phase of lethal irradiation. Importantly, preventing the formation of BM adipocytes alone

does not cause osteogenesis 15, indicating that osteogenesis requires simultaneous ablation of both the adipocytic and hematopoietic compartments. These data suggest a three-way co-regulation of hematopoiesis, osteogenesis and adipogenesis within the BM compartment.

Finally, we tested whether blocking adipogenesis pharmacologically could enhance bone marrow engraftment in wild-type mice. The PPARγ inhibitor Bisphenol-A-DiGlycidyl-Ether (BADGE) has been shown to prevent bone marrow adipocyte formation *in vitro* and *in vivo* in models of streptozotocin-induced diabetes 9, 15 . Importantly, BADGE does not enhance hematopoietic colony formation *in vitro*, when BM cells are isolated from their stromal microenvironment (supplementary figure 10). We administered BADGE to lethally irradiated mice for the two weeks following bone marrow transplantation, and observed successful inhibition of BM adipocyte formation (figure 4a), higher peripheral blood leukocyte counts (figure 4b), and an enrichment in colony forming units (figure 4c). Our results demonstrate that the negative influence of adipocytes on post-transplant hematopoietic engraftment can be overcome pharmacologically, and suggest that PPARγ inhibitors, or other adipocyte inhibitors such as the novel aP2 inhibitor BMS309403 16, might serve as adjuvants to hematopoietic recovery in clinical bone marrow transplantation.

Collectively, our results contradict the classical dogma that adipocytes act as passive space fillers in the marrow. We demonstrate that adipocyte-rich marrow harbors a decreased frequency of progenitors and relatively quiescent stem cells. Moreover, we observe that mice that are genetically deficient in adipogenesis show accelerated hematopoietic recovery after bone marrow ablation, a phenomenon that can be reproduced pharmacologically in wild-type mice through PPARγ inhibition. These results suggest a novel therapeutic approach to enhance hematopoietic engraftment following marrow or cord blood transplantation, or to ameliorate aplasia in genetic bone marrow failure syndromes. Furthermore, our results suggest a plausible mechanism for the reports of myelosuppression17, 18, 19 in patients treated with the PPARγ agonist rosiglitazone, a diabetes drug known to increase marrow adiposity 20.

Our data indicate a predominantly suppressive influence of adipocytes on hematopoiesis within the bone marrow microenvironment. BM adipocytes are less supportive of hematopoiesis *in vitro* than their undifferentiated stromal or pre-adipocytic counterparts, in part due to reduced production of growth factors such as GM-CSF and G-CSF 21, 22 . Moreover, adipose tissue secretes neuropillin-1 23, lipocalin 2 24, 25, adiponectin 26 and TNFalpha 27, 28 , each of which can impair hematopoietic proliferation. Of note, TNFalpha and adiponectin inhibit progenitor activity while positively influencing the most primitive HSCs 27, 29, suggesting that adipocytes prevent hematopoietic progenitor expansion while preserving the hematopoietic stem cell pool. Adipocytes and osteoblasts originate from mesenchymal stem cells within the bone marrow, where both compartments hold a reciprocal relationship 30. Balancing the supportive role of the osteoblast in the HSC niche, our data implicate adipocytes as negative regulators of hematopoiesis. Further studies will address the molecular players involved in the hematopoietic inhibition imposed by fatty marrow.

Methods Summary

Thorax, tibias and tails were isolated from wildtype C57BL6/J mice. B6.SJL-Ptprca Pep3b/BoyJ were used as bone marrow donors to exploit the CD45.1/CD45.2 allelic system (Jackson Laboratoriess #0002014). Bone marrow transplantation and CFU-Spleen assays were performed on lethally irradiated mice (two 5.5Gy doses separated by 3hrs) and cells were administered by tail vein injection within 24hrs of lethal irradiation. For competitive transplantation, samples were competed against 250,000 recipient-matched competitor

femoral bone marrow. FVB wildtype litter-mates mice were used as controls for FVB.A-ZIP/F1 fatless mice. During BM transplantation assays FVB or FVB.A-ZIP/F1 mice (CD45.1) received 200,000 MHC-matched (H^q) wildtype BM from DBA/1J mice (CD45.2). Secondary transplants were performed through recovery of the CD45.2 DBA/2 BM passed through the FVB wildtype or FVB.A-ZIP/F1 microenvironment, which was then transplanted into FVB (CD45.1) recipients together with 250,000 FVB (CD45.1) wildtype competitor BM cells. For pharmacological inhibition of adipocyte formation, BM transplants were performed in wild-type female FVB mice as described above, except that 30mg/kg BADGE or control vehicle (DMSO 10%) were administered in daily intraperitoneal injections starting one day prior to irradiation and continuing until day 14 post-transplant. 500mg BADGE (Fluka) was resuspended in 8.3ml DMSO (Sigma) and diluted in PBS to a final concentration of 10% DMSO for administration at 30mg/kg in 100ul. Aliquots were stored at −20°C and thawed daily. Multicolor flow cytometry was performed in a BD five-laser LSRII flow cytometer. Cell cycle analysis was performed with DAPI (Sigma) in cells fixed in 2% paraformaldehyde for 15 min at 4°C. For all statistical analysis un-paired two-tailed Student's t-test was performed assuming equal variance of samples. Error bars and confidence intervals represent the standard error of the mean (SEM) unless otherwise indicated.

Methods

Animals

All mice were purchased from Jackson Laboratories and sex, weight and age-matched or breeding colonies were established in house. Experiments were carried out with IACUC approval from CHB.

Bone marrow preparations

Femurs, thorax and tails were isolated free of muscle and tendons; when appropriate, the spinal cord was carefully removed. Bones were crushed in IMDM with mortal and pestle, filtered through a 70-μm filter and washed with PBS. A sample was removed, stained with CD45-FITC (1:200) and 7-AAD (1:100) in 50 ul and the volume raised to 500ul with PBS and reference beads (Sigma). A viable CD45+ cell count was then obtained with a F500-Coulter flow cytometer. Red blood cells from bone marrow in homeostatic conditions (pre-transplant) were lysed with RBC lysis buffer (Sigma). For early post-transplant analysis, BM was not lysed and efforts were made to perform minimal manipulation before CFU plating or secondary transplantation (RBCs were excluded as counts were based on CD45+ cells only).

Flow cytometry

Multicolor analysis for progenitor and stem cell quantification was performed on a FACS-Aria+UV or on a 5-laser-LSRII flow cytometer (BD). Cells were stained in PBS 2% FCS for 1 hour with CD34-FITC (1:50, BD), Flk2-PE (1:100, BD), Lineage cocktail-PECy5 (Ter119/B220/CD19/CD3/CD4/CD8/Nk1.1 from eBiosciences; mixed 1:1 except CD3 2:1, and used 1:200), FcγRIII/II-PECy7 (1:200, Biolegend), ckit-APC (1:200, BD), CD45.1 or CD45.2-APCCy7 (1:100, Biolegend), CD45-biotin (1:200, BD), Streptavidin-Pacific Orange (1:2000, Invitrogen), and Sca1-Pacific Blue (1:100 Biolegend). For cell cycle analysis, bone marrow cells were stained in cold 2%IFS and fixed in cold 2% PFA for 15 minutes, then washed, stained in DAPI solution for 10 minutes at room temperature (0.1% (v/v) Triton X-100 and 1 μg/ml DAPI in PBS [41,42]), washed and immediately analyzed. Ki-67 analysis was done as described by Wilson et al.31. Bone marrow cells were stained by cell surface markers (Sca1-FITC (1:100, BD), Lineage-cocktail (1:200), FcγRIII/II-PECy7 (1:200, Abcam), ckit-APC (1:200), CD45-APCCy7 (1:100, BD), CD150-biotin (1:300,

BioLegend), Streptavidin-Alexa Fluor 680 (1:200, Invitrogen)), washed, fixed in cold Cytofix/Cytoperm buffer (BD) for 20 minutes, then washed and incubated in Permwash buffer (BD) with Ki-67-PE (1:100, BD) for 5 hours at 4°C. Cells were treated with 1 μg/ml DAPI for 10 minutes, washed and resuspended in PBS 2% FCS immediately prior to acquisition.

Progenitor assays

Colony forming unit (CFU) assays were performed in complete M3434 methylcellulose (Stem Cell Technologies) following the manufacturer's instructions. Colonies were scored on day 8–10 on coded plates for unbiased counts.

Bone marrow transplantation

Mice were lethally irradiated with 11-12Gy split-dose 2.5hrs apart, and BM transplants performed within 24h by tail-vein injection. Engraftment was measured monthly through eye bleed and FACS analysis with CD45.1-FITC (eBiosciences), CD45.2-PE or CD45.2-biotin, CD3-PE, CD19-PE, Mac-1-PE. Gr1-PE, F4/80-APC. All antibodies were ordered from Beckton-Dickinson unless otherwise specified. Mice whose engraftment was below 0.5% were considered non-engrafted and were not taken into account for calculation of competitive repopulation units.

Stromal cell culture and differentiation

OP9 cells (ATCC) were expanded in MEMalpha 15%IFS + pen/strep/glutamine (Gibco); media changed every 3–4 days. Adipocytic differentiation was performed on confluent OP9s plated at 10,000/cm^2 with isobutylmethylxantine 0.5mM (IBMX, Sigma 1000x stock in DMSO), insulin 5ug/ml (Sigma, 1000x stock in PBS) and dexamethasone 10e-6M (Sigma, 1000x stock in ethanol) on the first week, then maintained with insulin and dexamethasone only for another 10 days Media changes were made every 3–4 days with fresh aliquots maintained in the dark at −20°C. Hematopoietic co-cultures with FACS-sorted ckit+Lin-Sca1+ (KLS) hematopoietic stem cells were performed in IMDM 10% IFS at 37°C and 5%CO2; media was changed on the seventh day of co-culture. For co-cultures, 2000 KLS cells were plated per well. Transwell assays used 12mm polyester inserts with 0.4μm pore size (Corning) with adipocytic or undifferentiated OP9 cells plated in the bottom of the plate while undifferentiated OP9s were co-cultured with KLS in the upper insert.

MicroPET analysis

For micro Positron Emission Tomography (mPET), mice were administered equal doses (5.6–9.3 MBq) of sodium fluoride-18 (F-18) by tail-vein injection. Animals were imaged prior to bone marrow transplantation, and the same cohort of animals was re-assayed at different times post-transplant. Exactly 30min after the F-18 injection, mice were imaged with a Focus 120 microPET scanner (Siemens). For normalization, the total dose injected was determined immediately pre- and post-imaging by introducing the anesthesized mouse in the dose calibrator and calculating the mid-acquisition dose as the average of the pre- and post-acquisition measurements adjusted by time decay. ASIPro software (Siemens) was then used for image analysis. To determine the F-18 uptake in tibias and tails, a 3D ROI (region of interest) was created in transverse sections through the selection of six 9×9 pixel planes moving distally from the tibial plate or 12 planes moving distally from the beginning of the free tail. The mean dose in the ROI (Bq/ml) was then normalized to the total injected dose and the ratios from pre to post-transplant F18-uptake were then calculated. When the whole cohort of mice could not be assayed on the same day post-transplant, data from the two closest dates was interpolated.

MicroCT analysis

For high-resolution micro Computerized Tomography (mCT) analysis, tibias were dissected, fixed in 10% formalin, and imaged with the Siemens microCAT II system.using a 22.75 micrometer pixel size. Beam angle of increment was 1 degree and tube voltage and current were 80 kvp and 450 μA per view as described by Botolin et al. [44]. Each run included wildtype and fatless bones and a calibration phantom to calibrate grayscale values with respect to mass density and maintain consistency. A fixed density threshold was established through normalization to the phantom to separate trabecular bone from bone marrow (1350 mg/ml). Trabecular bone analyses were done with ImageJ and AMIRA image analysis software in a 0.2mm thick 3D square region of trabecular bone defined at 1 mm under the growth plate of the proximal tibia extending 0.9 mm toward the diaphysis and excluding the outer cortical shell.

Supplementary Material

Refer to Web version on PubMed Central for supplementary material.

Acknowledgments

We thank Suzan Lazo-Kallanian, John Daley (Dana Farber Cancer Institute) and Grigoryi Losyev and Ronald Mathieu (Children's Hospital) for assistance with Flow Cytometry; Roderick Bronson (Harvard University) for assistance with pathological analysis; Patricia Dunning, Erin Snay and Stacey Carlton (Children's Hospital) for assistance with small animal imaging; Shannon McKinney-Freeman, Akiko Yabuuchi, Kitwa Ng, and Robert Chapman for mouse and technical assistance. O.N. was partially funded by the Barrie de la Maza Foundation. G.Q.D was supported by grants from the National Institutes of Health (NIH), and the NIH Director's Pioneer Award of the NIH Roadmap for Medical Research. GQD is the recipient of the Clinical Scientist Award in Translational Research from the Burroughs Wellcome Fund and the Leukemia and Lymphoma Society, and is an Investigator of the Howard Hughes Medical Institute.

References

1. Calvi LM, Adams GB, Weibrecht KW, Weber JM, Olson DP, et al. Osteoblastic cells regulate the haematopoietic stem cell niche. Nature. 2003; 425:841–846. [PubMed: 14574413]
2. Zhang J, Niu C, Ye L, Huang H, He X, et al. Identification of the haematopoietic stem cell niche and control of the niche size. Nature. 2003; 425:836–841. [PubMed: 14574412]
3. Kiel MJ, Yilmaz OH, Iwashita T, Terhorst C, Morrison SJ. SLAM family receptors distinguish hematopoietic stem and progenitor cells and reveal endothelial niches for stem cells. Cell. 2005; 121:1109–1121. [PubMed: 15989959]
4. Neumann E. Das Gesetz Verbreitung des gelben und rotten Markes in den Extremitätenknochen. Centralblatt für die medicinischen Wissenschaften. 1882; 18:321–323.
5. Calvo W, Fliedner TM, Herbst E, Hügl E, Bruch C. Regeneration of blood-forming organs after autologous leukocyte transfusion in lethally irradiated dogs. II. Distribution and cellularity of the marrow in irradiated and transfused animals. Blood. 1976; 47:593–601. [PubMed: 1260123]
6. Litten M, Orth J. Ueber Veränderungen des Marks in Röhrenknochen unter verschiedenen pathologischen Verhältnissen. Berliner klinische Wochenschrift. 1877; 51:743–751.
7. Bryon PA, Gentilhomme O, Fiere D. Histomorphometric analysis of bone-marrow adipose density and heterogeneity in myeloid aplasia and dysplasia. Pathol Biol (Paris). 1979; 27:209–213. [PubMed: 379758]
8. Moitra J, Mason MM, Olive M, Krylov D, Gavrilova O, et al. Life without white fat: a transgenic mouse. Genes Dev. 1998; 12:3168–3181. [PubMed: 9784492]
9. Wright HM, Clish CB, Mikami T, Hauser S, Yanagi K, et al. A synthetic antagonist for the peroxisome proliferator-activated receptor gamma inhibits adipocyte differentiation. J Biol Chem. 2000; 275:1873–1877. [PubMed: 10636887]

10. Christensen JL, Weissman IL. Flk-2 is a marker in hematopoietic stem cell differentiation: a simple method to isolate long-term stem cells. Proc Natl Acad Sci USA. 2001; 98:14541–14546. [PubMed: 11724967]
11. Osawa M, Hanada K, Hamada H, Nakauchi H. Long-term lymphohematopoietic reconstitution by a single CD34-low/negative hematopoietic stem cell. Science. 1996; 273:242–245. [PubMed: 8662508]
12. Pan Z, Yang J, Guo C, Shi D, Shen D, et al. Effects of hindlimb unloading on ex vivo growth and osteogenic/adipogenic potentials of bone marrow-derived mesenchymal stem cells in rats. Stem Cells Dev. 2008; 17:795–804. [PubMed: 18710346]
13. Yang L, Bryder D, Adolfsson J, Nygren J, Månsson R, et al. Identification of Lin(−) Sca1(+)kit(+)CD34(+)Flt3-short-term hematopoietic stem cells capable of rapidly reconstituting and rescuing myeloablated transplant recipients. Blood. 2005; 105:2717–2723. [PubMed: 15572596]
14. Tavassoli M, Maniatis A, Crosby WH. Induction of sustained hemopoiesis in fatty marrow. Blood. 1974; 43:33–38. [PubMed: 4809095]
15. Botolin S, McCabe LR. Inhibition of PPARgamma prevents type I diabetic bone marrow adiposity but not bone loss. J Cell Physiol. 2006; 209:967–976. [PubMed: 16972249]
16. Furuhashi M, Tuncman G, Görgün CZ, Makowski L, Atsumi G, et al. Treatment of diabetes and atherosclerosis by inhibiting fatty-acid-binding protein aP2. Nature. 2007; 447:959–965. [PubMed: 17554340]
17. Digman C, Klein AK, Pittas AG. Leukopenia and thrombocytopenia caused by thiazolidinediones. Ann Intern Med. 2005; 143:465–466. [PubMed: 16172449]
18. Maaravi Y, Stessman J. Mild, reversible pancytopenia induced by rosiglitazone. Diabetes Care. 2005; 28:1536. [PubMed: 15920093]
19. Berria R, Glass L, Mahankali A, Miyazaki Y, Monroy A, et al. Reduction in hematocrit and hemoglobin following pioglitazone treatment is not hemodilutional in Type II diabetes mellitus. Clin Pharmacol Ther. 2007; 82:275–281. [PubMed: 17361126]
20. Lazarenko OP, Rzonca SO, Hogue WR, Swain FL, Suva LJ, Lecka-Czernik B. Rosiglitazone induces decreases in bone mass and strength that are reminiscent of aged bone. Endocrinology. 2007; 148:2669–2680. [PubMed: 17332064]
21. Nishikawa M, Ozawa K, Tojo A, Yoshikubo T, Okano A, et al. Changes in hematopoiesis-supporting ability of C3H10T1/2 mouse embryo fibroblasts during differentiation. Blood. 1993; 81:1184–1192. [PubMed: 7680242]
22. Corre J, Barreau C, Cousin B, et al. Human subcutaneous adipose cells support complete differentiation but not self-renewal of hematopoietic progenitors. J Cell Physiol. 2006; 208:282–288. [PubMed: 16619234]
23. Belaid-Choucair Z, Lepelletier Y, Poncin G, Thiry A, Humblet C, et al. Human bone marrow adipocytes block granulopoiesis through neuropilin-1-induced granulocyte colony-stimulating factor inhibition. Stem Cells. 2008; 26:1556–1564. [PubMed: 18388301]
24. Miharada K, Hiroyama T, Sudo K, Danjo I, Nagasawa T, Nakamura Y. Lipocalin 2-mediated growth suppression is evident in human erythroid and monocyte/macrophage lineage cells. J Cell Physiol. 2008; 215:526–537. [PubMed: 18064607]
25. Yan QW, Yang Q, Mody N, Graham TE, Hsu CH, et al. The adipokine lipocalin 2 is regulated by obesity and promotes insulin resistance. Diabetes. 2007; 56:2533–2540. [PubMed: 17639021]
26. Yokota T, Oritani K, Takahashi I, Ishikawa J, Matsuyama A, Ouchi N, et al. Adiponectin, a new member of the family of soluble defense collagens, negatively regulates the growth of myelomonocytic progenitors and the functions of macrophages. Blood. 2000; 96:1723–1732. [PubMed: 10961870]
27. Zhang Y, Harada A, Bluethmann H, Wang JB, Nakao S, et al. Tumor necrosis factor (TNF) is a physiologic regulator of hematopoietic progenitor cells: increase of early hematopoietic progenitor cells in TNF receptor p55-deficient mice in vivo and potent inhibition of progenitor cell proliferation by TNF alpha in vitro. Blood. 1995; 86:2930–2937. [PubMed: 7579385]
28. Hotamisligil GS, Shargill NS, Spiegelman BM. Adipose expression of tumor necrosis factor-alpha: direct role in obesity-linked insulin resistance. Science. 1993; 259:87–91. [PubMed: 7678183]

29. DiMascio L, Voermans C, Uqoezwa M, Duncan A, Lu D, et al. Identification of adiponectin as a novel hemopoietic stem cell growth factor. J Immunol. 2007; 178:3511–3520. [PubMed: 17339446]

30. Nuttall ME, Gimble JM. Controlling the balance between osteoblastogenesis and adipogenesis and the consequent therapeutic implications. Curr Opin Pharmacol. 2004; 4:290–294. [PubMed: 15140422]

31. Wilson A, Murphy MJ, Oskarsson T, Kaloulis K, Bettess MD, Oser GM, et al. c-Myc controls the balance between hematopoietic stem cell self-renewal and differentiation. Genes Dev. 2004; 18:2747–2763. [PubMed: 15545632]

32. Pozarowski P, Darzynkiewicz Z. Analysis of cell cycle by flow cytometry. Methods Mol Biol. 2004; 281:301–311. [PubMed: 15220539]

33. Goodell MA, Brose K, Paradis G, Conner AS, Mulligan RC. Isolation and functional properties of murine hematopoietic stem cells that are replicating in vivo. J Exp Med. 1996; 83:1797–1806. [PubMed: 8666936]

34. Botolin S, McCabe LR. Inhibition of PPARgamma prevents type I diabetic bone marrow adiposity but not bone loss. J Cell Physiol. 2006; 209:967–976. [PubMed: 16972249]

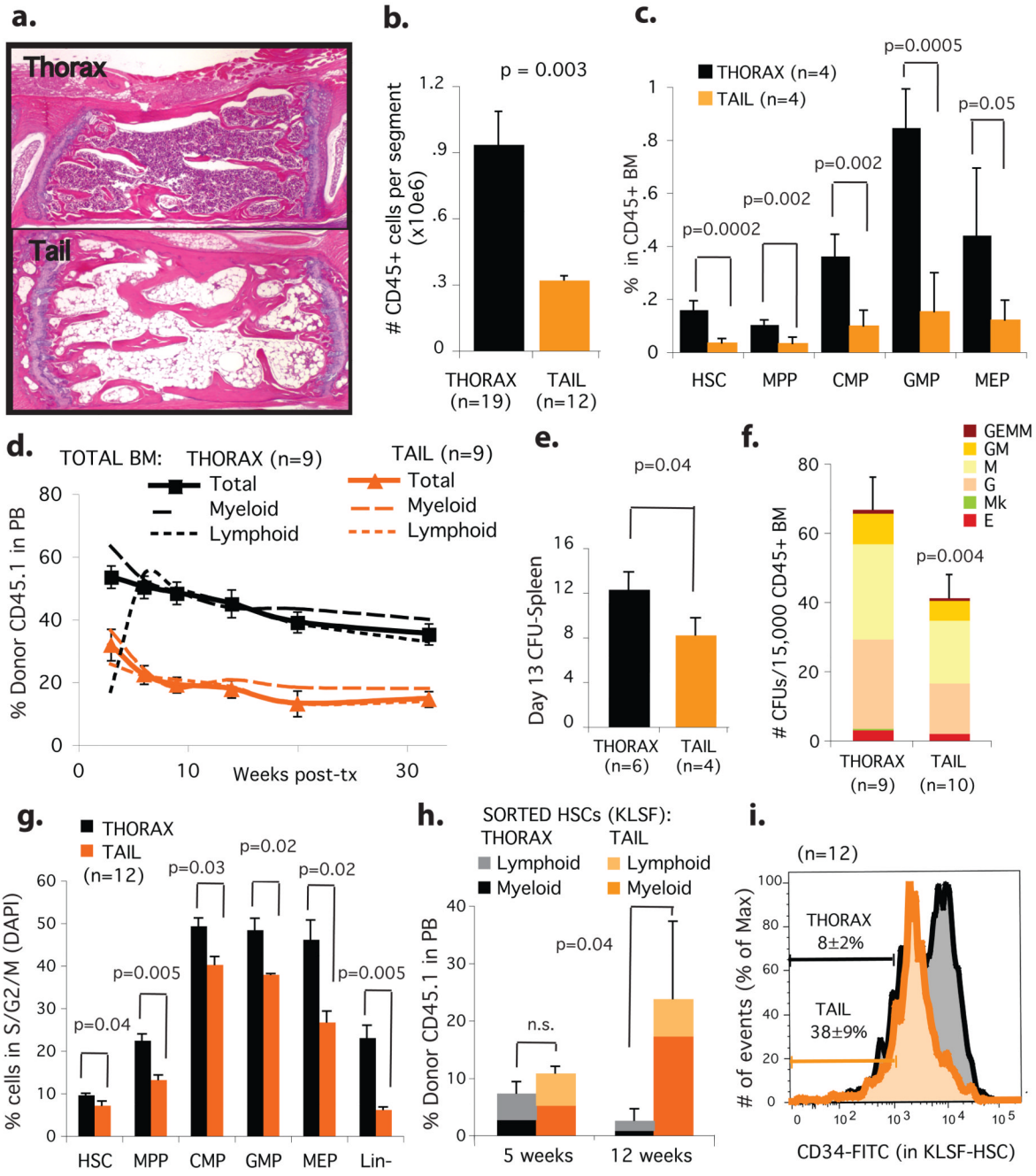

Figure 1. Hematopoietic stem cells and progenitors are reduced in number, frequency and cycling capacity in adipocyte-rich bone marrow during homeostasis

a.H&E-stain of decalcified thoracic vertebra (top) and fourth-tail-segment (bottom), 12-week-old C57BL/6J mice. **b.**Absolute number of hematopoietic cells (CD45+) per vertebral segment. **c.**Progenitor frequency within the hematopoietic compartment (CD45+). **d.**Competitive engraftment (250,000 CD45.1 tail or thorax BM; 250,000 CD45.2 competitor BM), **e.**Day 13 spleen-colony assay, and **f.**CFU-progenitor assay from tail and thorax BM. **g.**Progenitor cell cycle analysis .average % cells in S/G2/M transition ± SEM. **h.**100 tail and thorax BM sorted HSC (ckit+Lin-Sca1+Flk2−; >95% purity) were transplanted competitively, then engraftment in peripheral blood monitored. **i.**CD34 expression within

the HSC fraction (KLSF, ckit+Lin-Sca1+Flk2−); % CD34low within KLSF fraction indicated.

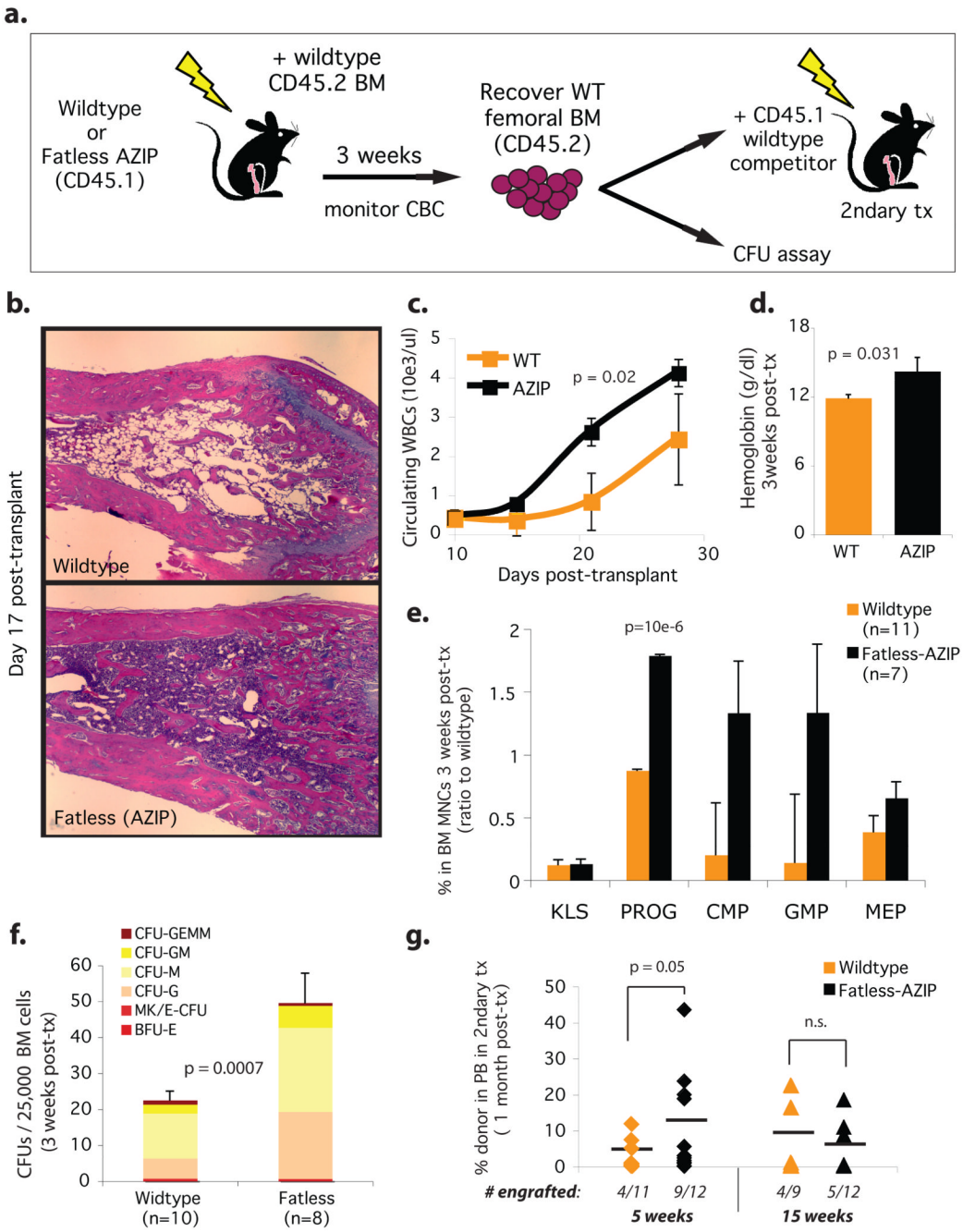

Figure 2. The lack of bone marrow adipocytes post-irradiation in fatless mice enhances hematopoietic progenitor expansion and post-transplant recovery

a.Experimental design. Wildtype FVB or fatless FVB.A-ZIP/F 16-week-old mice (CD45.1) were lethally irradiated and transplanted with 200,000 CD45.2, MHC-compatible DBA/1 wild-type BM. Femurs were isolated on day 17–20 post-transplant and donor DBA CD45.2 wildtype BM was recovered by high purity FACS, then used for progenitor assays or competitive serial transplantation. **b.**Femoral H&E in the third week post-transplant. **c.**White blood cell (WBC) counts and **d.**hemoglobin levels in peripheral blood after primary transplant. BM recovered from primary transplants was assayed for **e.**relative frequency of

progenitors by FACS (± STD) **f.**colony forming units assay (CFU), and **g.**secondary competitive transplantation into wildtype recipients.

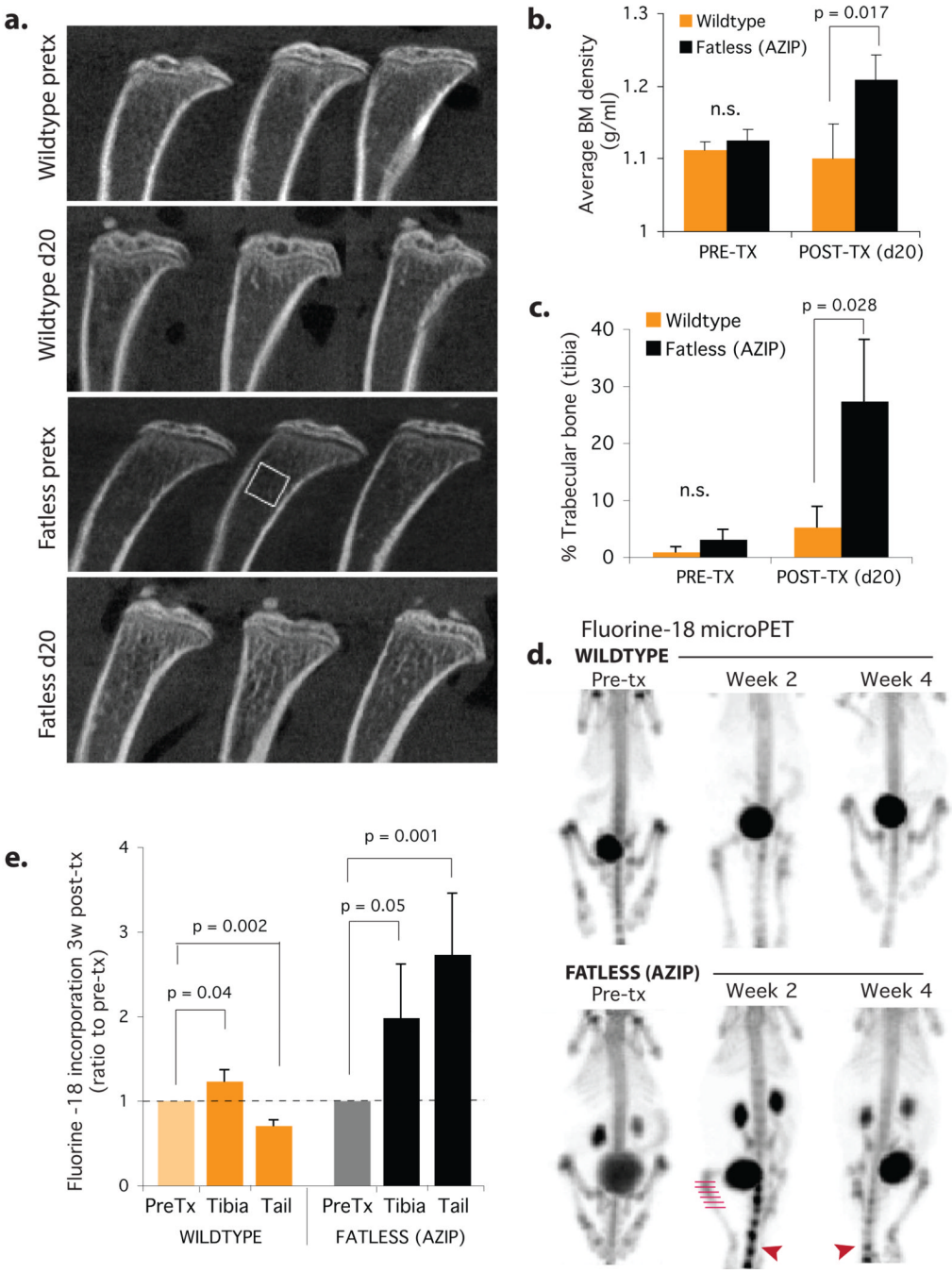

Figure 3. Ablation of the hematopoietic compartment in fatless A-ZIP/F1 mice during BM transplantation induces osteogenesis

Analysis of mice transplanted as in figure 2. **a.**High-resolution microCT analysis of pre/post-transplant tibias from wildtype (top) or fatless A-ZIP/F1 mice 20 days after lethal ablation. **b.**Average trabecular bone density of (**a**) normalized to a density standard (phantom). **c.**Percentage BM space occupied by trabecular bone 20 days after transplantation. **d.**MicroPET analysis pre/post-transplant. Representative mice shown at three different timepoints (3–4 analyzed per group). Dark areas indicate NaF-18 uptake in regions of active bone deposition (red arrowheads). **e.**Quantification of mean NaF-18 uptake

in tibiae and proximal tails pre/post-transplantation. Square and lines over micrographs **a.** and **d.** indicate quantification regions (see methods).

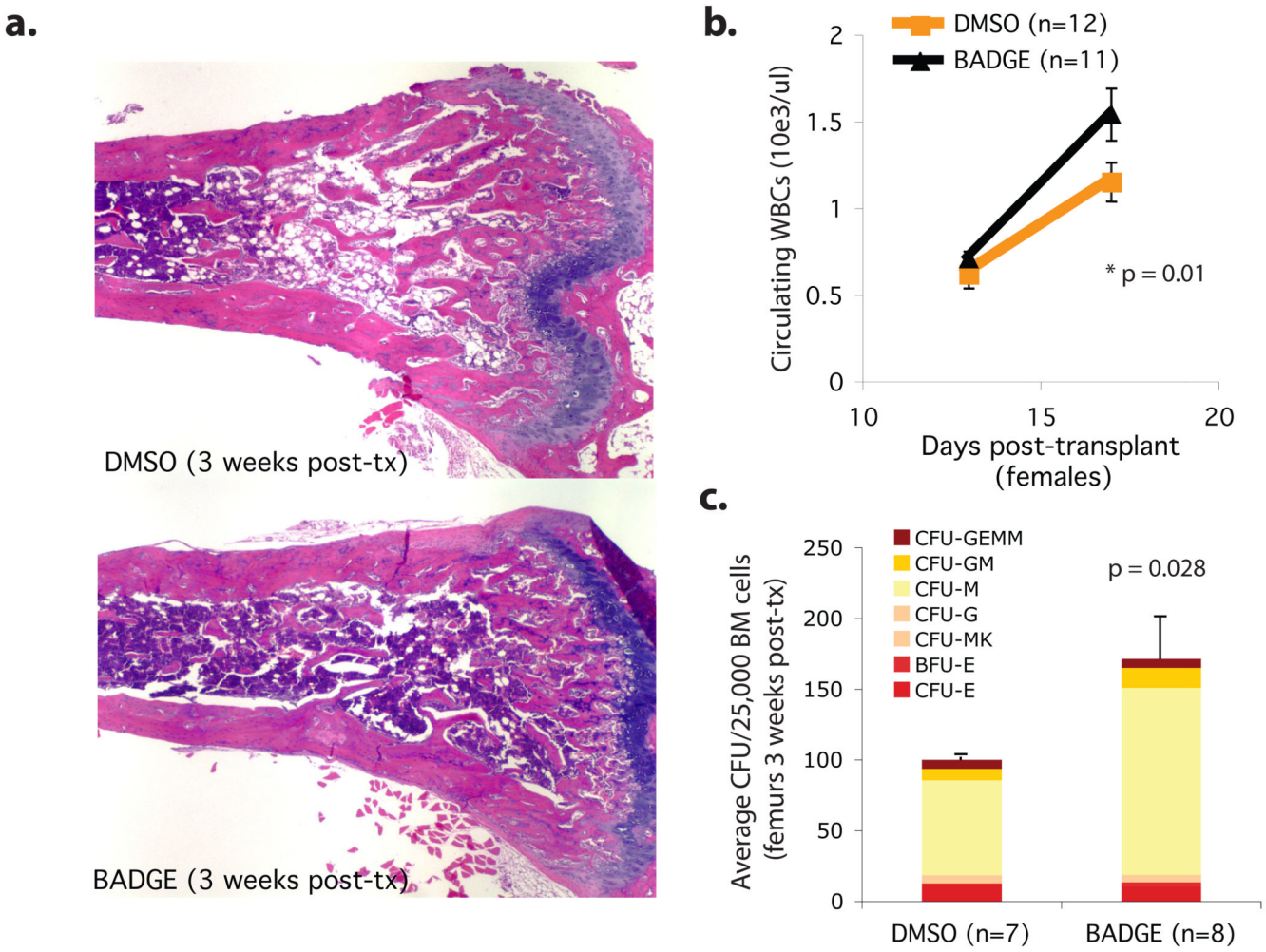

Figure 4. Pharmacological inhibition of adipocyte formation enhances BM engraftment in wild-type mice

BM transplants were performed in wild-type female FVB mice as described for figure 2 except that 30mg/kg BADGE or control vehicle (DMSO 10%) were administered through daily intra-peritoneal injections from the day prior to irradiation until day 14 post-transplant. **a.**H&E stain of femurs from mice sacrificed on day 17 post-transplant, when the donor CD45.2 wildtype BM was recovered and purified by FACS. **b.**White blood cell (WBC) counts in peripheral blood on the post-transplant period show accelerated recovery in BADGE-treated mice. **c.**Colony forming unit assay (CFU) from the recovered donor BM